

DEUTSCHES ELEKTRONEN-SYNCHROTRON **DESY**

DESY 82-003
January 1982

PRODUCTION OF HEAVY RESONANCES
WITH ELECTRON AND MUON BEAMS

by

J. G. Körner

Deutsches Elektronen-Synchrotron DESY, Hamburg

J. Cleymans and M. Kuroda

University of Bielefeld

G. J. Gounaris

University of Thessaloniki

NOTKESTRASSE 85 · 2 HAMBURG 52

DESY behält sich alle Rechte für den Fall der Schutzrechtserteilung und für die wirtschaftliche Verwertung der in diesem Bericht enthaltenen Informationen vor.

DESY reserves all rights for commercial use of information included in this report, especially in case of apply for or grant of patents.

**To be sure that your preprints are promptly included in the
HIGH ENERGY PHYSICS INDEX ,
send them to the following address (if possible by air mail) :**

**DESY
Bibliothek
Notkestrasse 85
2 Hamburg 52
Germany**

PRODUCTION OF HEAVY RESONANCES
WITH ELECTRON AND MUON BEAMS

by

J.G.Körner, J.Cleymans, M.Kuroda and G.J.Counaris

ERRATUM

p. 9 Eq.(24) : $\sum_{i=1}^q \rightarrow \sum_{i=1}^q$

p. 11 Eq.(27) : $\Psi(o) \rightarrow \Psi(o)^*$

p. 19 8th and 9th line should read :

- target frame: $-\vec{g}_1$ along z-axis ($\Theta_1 = \pi$)
- recoil frame: $-(\vec{Q} + \frac{\vec{g}_1}{3})$ along z-axis

p. 24 Eq.(A7) should read :

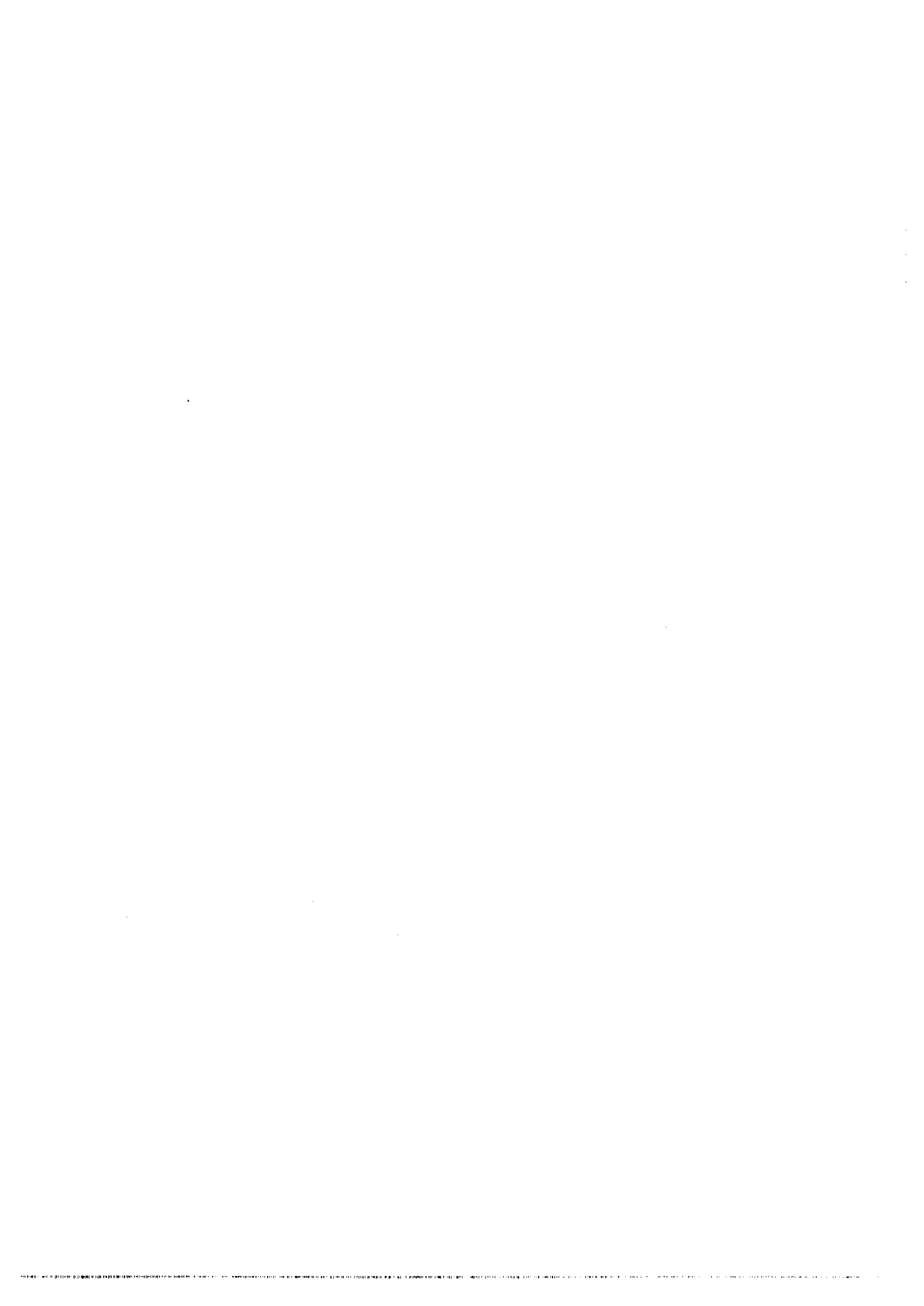
$$\Theta_1^T = \pi ; \quad \Theta_2^T = \pi + \Theta_2 - \Theta_1 ; \quad \Theta_q^T = \pi + \Theta_q - \Theta_1$$

p. 25 Eq.(A8) should read :

$$\Theta_2^R = \pi - \Theta_R ; \quad \Theta_1^R = \pi + \Theta_1 - \Theta_2 - \Theta_R ; \quad \Theta_q^R = \pi + \Theta_q - \Theta_2 - \Theta_R$$

4th line: $\Theta_2^R \rightarrow \Theta_R$

p. 26 Ref. 1: 365 \rightarrow 364



Abstract

The inelastic leptonproduction of heavy resonances J ($J = J/\psi, Y, \dots$) is investigated in a model where $\gamma, g \rightarrow Jg$ is assumed to be the dominant mechanism. Analytic expressions for the differential cross section as well as for the helicity amplitudes are presented. A detailed numerical analysis of the angular distribution of the muon pair arising from the decay of the heavy resonance in its rest frame is presented.

PRODUCTION OF HEAVY RESONANCES

WITH

ELECTRON AND MUON BEAMS

J. G. Körner

DESY, Hamburg, Germany

J. Cleymans and M. Kuroda⁺

University of Bielefeld, Germany

and

G. J. Gounaris

University of Thessaloniki, Greece

⁺) Supported by Deutsche Forschungsgemeinschaft

1. Introduction

The production of heavy resonances in hadronic reactions is widely assumed to arise from the collision of two constituents. A clean test of this idea is marred by the fact that in hadronic collisions many different diagrams make substantial contributions, for example, $gluon + gluon \rightarrow resonance + gluon$ ¹ or the direct fusion of two gluons into a P-wave resonance which subsequently decay into the J/ψ (or Υ) resonance plus a photon². Furthermore, at lower energies, more complicated diagrams having a quark and a gluon in the initial state are not negligible. One may however think that certain diagrams would dominate in specific regions of phase space, as for example the $gluon + gluon \rightarrow resonance + gluon$ mechanism may dominate at large transverse momenta over the gluon fusion mechanism with subsequent radiative decay². This is however limited to specific reactions in specific energy regions (it seems to be the case for Υ -production in pp collisions) and depends on the smearing in transverse momentum of the incoming constituents. Without smearing the gluon fusion mechanism limits values of the transverse momentum of the J/ψ by:

$$p_T^2 \leq \frac{(m_p^2 - m_{J/\psi}^2)^2}{4 m_p^2}$$

where m_p is the mass of the P-wave resonance. In the case of the J/ψ this means $p_T^2 \leq 0.18 \text{ GeV}^2$, indeed a very small region in p_T . This limit is however meaningless since smearing in the transverse momentum of the initial gluons may easily produce values above 1 GeV^2 .

For the above mentioned reasons it is of interest to look for production reactions which would uniquely single out one specific set of diagrams, thereby allowing a cleaner analysis of the production mechanism. Such a reaction exists in nature, namely, heavy resonances produced by photons³ and by electron or muon beams^{4,5} (see figure 1). In these cases the direct production of P-wave resonances is forbidden: a photon (virtual or real) cannot fuse with a gluon to form a resonance because it is not possible to balance colour between initial and final states. This eliminates a priori the diagram that contributes most to the production of heavy resonances in hadronic collisions. The main left-over diagram has a very nice structure: it is simply the diagram responsible for the gluonic decay of J/ψ (or Υ) with one of the gluons replaced by a photon and the appropriate crossings from the initial to the final state. As emphasized by Berger and Jones³ for the photoproduction cases one correctly

projects out the spin-1 part of the quark-antiquark final state and also takes into account the colour singlet nature of the heavy resonance. This approach therefore provides a more physically correct description of the production mechanism than other approaches, e.g. the open charm production mechanism implemented with duality to fix the magnitude of the cross-section⁶.

It is the purpose of the present paper to present a detailed analysis of the leptoproduction mechanism of heavy resonances, in particular, we concentrate on the angular distribution of the muon pair in the final state. It has been shown by Keung⁴ and by Baier and Rückl⁵ that the model based on the diagrams of figure 2 provides a good description of the Q^2 -dependence of the cross-section^{4,5}, of the energy dependence of the photoproduction cross-section^{4,5} of the z -dependence⁴ (z being the energy fraction of the virtual photon taken by the J/ψ), see equation (36) below) and of the t -dependence⁴ of the cross-section. Baier and Rückl⁵ also present predictions concerning the distribution in polar angle of one of the decay muons in the rest frame of the heavy resonance. Our analysis goes beyond these calculations since we present results on the polar and azimuthal angular distributions of the lepton pair in the decay of the heavy resonance. It turns out that by organizing the calculation properly one arrives at relatively compact analytic expressions for the desired distributions. These expressions may be useful for subsequent applications when more data become available. We furthermore present a complete numerical analysis of the angular distributions of the lepton pair arising from the decay of the heavy resonance. From a theoretical point of view we remark here that the frame having the recoil axis does not coincide with the recoil axis at the constituent level. The most natural choice is the virtual photon direction since this is common to both the constituent interaction and the hadronic interaction. This axis furthermore does not suffer from smearing effects in the transverse momentum direction, as would be the case if the momentum of the target (in the rest frame of the heavy resonance) were chosen as z -axis, a problem which seriously complicates the analysis of angular distributions in the Drell-Yan process and leads to the introduction of the Collins-Soper frame⁷ as a way of minimizing these effects. All these considerations are unnecessary if the virtual photon direction is chosen as z -axis. In our numerical calculations we have consistently integrated over the azimuthal angle of the plane formed by the incoming and scattered lepton.

In section II we present the most general form for the angular distribution.

In section III we present the calculations and analytic results based on the diagrams in figure 2.

In section IV we present the numerical results of our analysis and compare them with previous calculations.

In section V we collect our conclusions and comments.

II. General Formalism

In this section we study the inelastic production cross-section (figure 1) in a model-independent way. Most of the notations are defined in the figure.

We will denote the lepton current (ℓ_1, ℓ_2) by L :

$$L_{\mu} = \bar{u}(\ell_2) \gamma_{\mu} u(\ell_1), \quad (1)$$

and the muon current, from the decay of the heavy resonance, (k_1, k_2) by M :

$$M_{\mu} = \bar{u}(k_2) \gamma_{\mu} v(k_1). \quad (2)$$

To investigate the helicity structure of the general process one decomposes these currents into left-handed and right-handed parts. This decomposition is correct provided one neglects electron and muon masses. This approximation will be made in the rest of this paper. Equations (1) and (2) can thus be written as:

$$L_{\mu} = \frac{1}{2} \bar{u}(\ell_2) \gamma_{\mu} (1+\gamma_5) u(\ell_1) + \frac{1}{2} \bar{u}(\ell_2) \gamma_{\mu} (1-\gamma_5) u(\ell_1) = L_{\mu}^R + L_{\mu}^L, \quad (3)$$

$$M_{\mu} = \frac{1}{2} \bar{u}(k_2) \gamma_{\mu} (1+\gamma_5) v(k_1) + \frac{1}{2} \bar{u}(k_2) \gamma_{\mu} (1-\gamma_5) v(k_1) = M_{\mu}^R + M_{\mu}^L. \quad (4)$$

Each one of these currents is conserved (up to terms proportional to lepton masses). They can therefore be written in a basis of three orthogonal vectors: $\epsilon_{\mu}(\pm 1)$, $\epsilon_{\mu}(\pm 1)$ and $\epsilon_{\mu}(-1)$ corresponding to the polarizations of the associated photons. For the lepton current L_{μ} one has:

$$L_{\mu}^R(L) = \sqrt{\frac{-2Q^2 \epsilon}{1-\epsilon}} [\pm \epsilon_{\mu}(\pm 1) - \alpha_{\pm} \epsilon_{\mu}(\pm 1)] e^{\pm i\phi} - \alpha_{\pm} \epsilon_{\mu}(\pm 1) e^{\mp i\phi} \quad (5)$$

where, in a standard notation,

$$\epsilon = \frac{4 E_1 E_2 + Q^2}{2 E_1^2 + 2 E_2^2 - Q^2} \quad \text{and} \quad \alpha_{\pm} = \frac{\sqrt{1-\epsilon} \pm \sqrt{1+\epsilon}}{2\sqrt{\epsilon}} \quad (6)$$

with E_1 and E_2 the energies of the incident and scattered lepton (Q^2 is negative), while ϕ is the angle between the lepton plane (ℓ_1, ℓ_2) and the hadronic plane defined by Q and p_J (see figure 1).

For the muon current one has in the rest frame of the heavy resonance:

$$M_{\mu}^R(L) = M_J [\pm \sin \theta \epsilon_{\mu}(0) - \sqrt{2} \sin^2 \frac{\theta}{2} e^{\mp i\phi} \epsilon_{\mu}(\pm 1) - \sqrt{2} \cos^2 \frac{\theta}{2} e^{\pm i\phi} \epsilon_{\mu}(\mp 1)] \quad (7)$$

where θ and ϕ are the polar and azimuthal angles of one of the muons in the rest frame of J . M_J is the mass of the heavy resonance.

The general matrix element for the process of figure 1 is

$$M(\ell_1 + T \rightarrow \ell_2 + J + \text{hadrons}; J \rightarrow \mu^+ \mu^-) = \frac{e^2}{Q^2} L_{\mu}^R T_{\mu\nu} M_{\nu}^R \frac{1}{p_J^2 - p_J^2 - iM_J \Gamma_J} \quad (8)$$

In equation (8) we have taken out all the model independent factors like propagators and electromagnetic coupling constants and the hadronic dynamics is represented by $T_{\mu\nu}$. T denotes the target particle (proton or nucleus) and J the heavy resonance, $J = (J/\psi, Y, \dots)$. In the narrow resonance approximation, the modulus squared of the matrix element in (8) is:

$$\begin{aligned} & \sum_{\text{spins}} |M(\ell_1 + T \rightarrow \ell_2 + J + \text{hadrons}; J \rightarrow \mu^+ \mu^-)|^2 \\ &= \frac{e^4}{Q^4} \frac{\pi}{M_J^2} \frac{1}{M_J^2 \Gamma_J^2} \delta(p_J^0 - M_J^2) (L_{\mu}^R)^{\dagger} (L_{\mu}^R) + (L_{\mu}^L)^{\dagger} (L_{\mu}^L) \sum_{\text{spins}} T_{\mu\nu}^{\dagger} T_{\nu\mu} \\ & \quad (M_{\nu}^R)^{\dagger} (M_{\nu}^R) + (M_{\nu}^L)^{\dagger} (M_{\nu}^L) \end{aligned} \quad (9)$$

With the help of the decompositions (6) and (7) one can rewrite equation (9) into a form making the angular distributions explicit. To this end we define:

$$H_{JJ'}^{\lambda\lambda'} = \epsilon_{\mu}^{\lambda} \epsilon_{\mu'}^{\lambda'} \left(\sum_{\text{hadronic spins}} T_{\mu\nu}^{\lambda\lambda'} \epsilon_{\nu}^*(j) \epsilon_{\nu'}(j') \right) \quad (10)$$

where $\epsilon_{\mu}^{\lambda}(\epsilon)$ ($\epsilon_{\mu'}^{\lambda'}(\epsilon')$) refers to the polarization vector with helicity $\lambda(\lambda')$ of the incoming virtual photon while $\epsilon_{\nu}^*(j)$ ($\epsilon_{\nu'}(j')$) refers to the polarization vector with helicity $j(j')$ of the outgoing photon coupled to the muon pair. In expression (9) we now have:

$$\begin{aligned} & (L_{\mu}^{R+R} + L_{\mu}^{L+L}) \left(\sum_{\text{spins}} T_{\mu\nu}^{\lambda\lambda'} \right) (M_{\nu\nu'}^{R+R} + M_{\nu\nu'}^{L+L}) \\ &= \sum_{\lambda, \lambda'; j, j'} \rho_{\lambda\lambda'}(\epsilon, Q^2, \Phi) H_{JJ'}^{\lambda\lambda'} W_{jj'}(\theta, \phi) \end{aligned} \quad (11)$$

The virtual photon density matrix elements $\rho_{\lambda\lambda'}(\epsilon, Q^2, \Phi)$ depend on the virtuality Q^2 of the photon, on the azimuthal angle ϕ and on the parameter ϵ defined in (6). Its components can be deduced from (5) and are given by:

$$\rho_{++} = \rho_{--} = \frac{-Q^2}{2(1-\epsilon)} \quad (12a)$$

$$\rho_{00} = \frac{-\epsilon Q^2}{1-\epsilon} \quad (12b)$$

$$\rho_{+0} = (\rho_{0+})^* = -\rho_{0-} = -(\rho_{-0})^* = \frac{Q^2}{2(1-\epsilon)} e^{i\phi} \quad (12c)$$

$$\rho_{+-} = (\rho_{-+})^* = \epsilon \frac{Q^2}{2(1-\epsilon)} e^{2i\phi} \quad (12d)$$

The angular decay matrix $W_{JJ'}(\theta, \phi)$ depends on the rest frame polar and azimuthal angles θ and ϕ of the heavy resonance decaying into a back-to-back $\mu^+ \mu^-$ pair. Neglecting lepton masses one finds from (6):

$$W_{++} = W_{--} = \frac{3}{16\pi} (1 + \cos^2\theta) \quad (13a)$$

$$W_{00} = \frac{3}{8\pi} \sin^2\theta \quad (13b)$$

$$W_{+0} = (W_{0+})^* = -W_{0-} = - (W_{-0})^* = \frac{3}{16\sqrt{2}\pi} \sin^2\theta e^{i\phi} \quad (13c)$$

$$W_{+-} = (W_{-+})^* = -\frac{3}{16\pi} \sin^2\theta e^{2i\phi} \quad (13d)$$

We now perform the helicity summation in (11) in order to bring out the general

form of the angular distributions*. The summation considerably simplifies when the hermiticity and parity properties are used:

$$H_{JJ'}^{\lambda\lambda'} = H_{JJ'}^{\lambda'\lambda} \quad (\text{hermiticity}), \quad (14)$$

$$H_{JJ'}^{\lambda\lambda'} = \pm H_{-J-J'}^{\lambda\lambda'} \quad (\text{parity}). \quad (15)$$

In (15) the + (-) sign should be used for odd (even) number of longitudinal components.

$$\begin{aligned} & \sum_{j, j', \lambda, \lambda'} \rho_{\lambda\lambda'} H_{JJ'}^{\lambda\lambda'} W_{jj'} \\ &= ((H_{++}^{++} + H_{--}^{++})(1 + \cos^2\theta) + 2 H_{00}^{++} \sin^2\theta \\ &+ \text{Re}(H_{+0}^{++} - H_{-0}^{--}) \sqrt{2} \sin 2\theta \cos\phi \\ &+ 2 \text{Re} H_{+-}^{++} \sin^2\theta \cos 2\phi) + \\ &+ 2 \epsilon (H_{++}^{00} (1 + \cos^2\theta) + H_{00}^{00} \sin^2\theta + \sqrt{2} \text{Re} H_{+0}^{00} \sin 2\theta \cos\phi \\ &+ H_{+-}^{00} \sin^2\theta \cos 2\phi) \\ &- \epsilon \cos 2\phi \{ 2 \text{Re} H_{++}^{+-} (1 + \cos^2\theta) + 2 H_{00}^{+-} \sin^2\theta \\ &+ \sqrt{2} \text{Re} (H_{+0}^{+-} + H_{0+}^{+-}) \sin 2\theta \cos\phi \\ &+ (H_{+-}^{+-} + H_{-+}^{+-}) \sin^2\theta \cos 2\phi \} \\ &+ \epsilon \sin 2\phi \{ + \sqrt{2} \text{Re} (H_{+0}^{+-} - H_{0+}^{+-}) \sin 2\theta \cos\phi + (H_{+-}^{+-} - H_{-+}^{+-}) \sin^2\theta \cos 2\phi \} \\ &+ \sqrt{\epsilon(1+\epsilon)} \cos\phi \{ 2 \text{Re} (H_{++}^{+0} + H_{--}^{+0}) (1 + \cos^2\theta) + 4 \text{Re} H_{00}^{+0} \sin^2\theta \\ &+ \sqrt{2} \text{Re} (H_{+0}^{+0} + H_{0+}^{+0} - H_{-0}^{+0} - H_{0-}^{+0}) \sin 2\theta \sin\phi \\ &+ 2 \text{Re} (H_{+-}^{+0} + H_{-+}^{+0}) \sin^2\theta \cos 2\phi \} \\ &+ \sqrt{\epsilon(1+\epsilon)} \sin\phi \{ \sqrt{2} \text{Re} (H_{+0}^{+0} - H_{0+}^{+0} + H_{-0}^{+0} - H_{0-}^{+0}) \sin 2\theta \sin\phi \\ &+ 2 \text{Re} (H_{+-}^{+0} - H_{-+}^{+0}) \sin^2\theta \cos 2\phi \} \end{aligned} \quad (16)$$

*) Expression (16) below generalizes the result of Schilling and Wolf⁹ to the inelastic vector meson production process.

Equation (16) gives the most general structure for the angular dependence of the process under consideration. In the rest of this paper we will be concerned with the ϕ -integrated cross-section so that only the first two curly brackets will contribute*.

III. Constituent Model

a) Structure of the Model

The model we considered is described by the six diagrams in figure 2. These lead to the following expression for the amplitude $T_{\mu\nu}$ defined in (8):

$$T_{\mu\nu} = e^i e^j \epsilon^k \epsilon^l \epsilon^m \epsilon^n \left(\text{Tr} \frac{\lambda^a}{2} \frac{\lambda^b}{2} \right) g_s^2 [\psi(0) / 2M_J]^2 4 e_q^2 C_{\mu\nu\alpha\beta} \quad (17)$$

where e^i (e_q^j) is the polarization vector of the incoming (outgoing) gluon, $\frac{\lambda^a}{2}$ is the SU(3) color matrix, g_s is the gluon-quark coupling constant, $\psi(0)$ is the quark-antiquark binding wave function taken at the origin in coordinate space, e_q is the charge of the quark (i.e. either + 2/3 or - 1/3) and $C_{\mu\nu\alpha\beta}$ is given in the following expression:

$$\begin{aligned} C_{\mu\nu\alpha\beta} = & \text{Tr} \left\{ \gamma_\nu (\not{p} + m_C) \gamma_\mu \frac{\not{p} - \not{q} + m_C}{t + Q^2 - M_J^2} \gamma_\beta \frac{\not{p} - \not{q}_2 + m_C}{s - M_J^2} \gamma_\alpha \right. \\ & + \gamma_\nu (\not{p} + m_C) \gamma_\beta \frac{\not{p} - \not{q}_1 + m_C}{u - M_J^2} \gamma_\mu \frac{\not{p} - \not{q}_2 + m_C}{s - M_J^2} \gamma_\alpha \\ & + \gamma_\nu (\not{p} + m_C) \gamma_\mu \frac{\not{p} - \not{q} + m_C}{t + Q^2 - M_J^2} \gamma_\alpha \frac{\not{p} + \not{q}_1 + m_C}{u - M_J^2} \gamma_\beta \\ & + \gamma_\nu (\not{p} + m_C) \gamma_\beta \frac{\not{p} - \not{q}_1 + m_C}{u - M_J^2} \gamma_\alpha \frac{\not{p} + \not{q}_2 + m_C}{t + Q^2 - M_J^2} \gamma_\mu \\ & + \gamma_\nu (\not{p} + m_C) \gamma_\beta \frac{\not{p} - \not{q}_1 + m_C}{u - M_J^2} \gamma_\mu \frac{\not{p} - \not{q}_2 + m_C}{s - M_J^2} \gamma_\alpha \\ & \left. + \gamma_\nu (\not{p} + m_C) \gamma_\mu \frac{\not{p} - \not{q} + m_C}{t + Q^2 - M_J^2} \gamma_\beta \frac{\not{p} - \not{q}_2 + m_C}{s - M_J^2} \gamma_\alpha \right\} \quad (18) \end{aligned}$$

*) The t -dependence has been investigated in a different model in references 10 and 11.

The traces in (18) appear already at the amplitude level because one requires the quark-antiquark wave function to be in a $J = 1$ state, e.g. for spin up:

$$v(+)\bar{u}(+) = \frac{1}{\sqrt{2}} \epsilon(+)(\not{p} + m_C) \quad (19)$$

each constituent carrying half of the resonance momentum. In equation (18) we introduced the variables p , s , t , u , and m_C , these are defined as follows:

$$p \approx \frac{1}{2} P_J \quad (20a)$$

$$s \equiv (g_1 + Q)^2 \quad (20b)$$

$$t \equiv (Q - p_J)^2 \quad (20c)$$

$$u \equiv (P_J - g_1)^2 \quad (20d)$$

and m_C is the mass of the constituent quark, taken as approximately equal to $M_J/2$.

After taking the modulus squared of the amplitude for the process at the constituent level we sum over the spins and colors of the incoming particles and take the average for the outgoing ones. This leads us to:

$$\begin{aligned} \frac{1}{4} \cdot \frac{1}{8} \sum_{\text{spins}} \sum_{\text{colour}} |M(l_1 + g_1 \rightarrow l_2 + J + g_2; J \rightarrow \mu^+ \mu^-)|^2 \\ = \frac{64 \alpha_s^4 \alpha_c^2 (4\pi)^6 e_q^4}{Q^4 M_J^2 \Gamma_J} |\psi(0)|^4 \pi \delta(p_J^2 - M_J^2) \\ L_{\mu\mu'} M_{\nu\nu'} C_{\mu\nu\alpha\beta} C_{\mu'\nu'\alpha\beta} \quad (21) \end{aligned}$$

where $L_{\mu\mu'}$ and $M_{\nu\nu'}$ arise from squaring and spin-averaging the lepton and muon currents:

$$L_{\mu\mu'} \equiv k_{1\mu} k_{2\mu'} + k_{1\mu'} k_{2\mu} + \frac{1}{2} Q^2 g_{\mu\mu'} \quad (22)$$

$$M_{\nu\nu'} \equiv k_{1\nu} k_{2\nu'} + k_{1\nu'} k_{2\nu} - \frac{1}{2} M_J^2 g_{\nu\nu'} \quad (23)$$

The evaluation of the r.h.s of (21) will be presented now in which the angular distribution given in (16) is implicit.

b) Explicit Expressions for the Constituent Process

Calculating the traces in (18), squaring the whole expression and then finally multiplying with (22) and (23) leads to a very large number of terms. After rearranging the expressions, we are left with the following:

$$\begin{aligned} & L_{\mu\nu} M_{\nu\nu'} C_{\mu\nu\alpha\beta} C_{\mu'\nu'\alpha\beta} \\ &= \frac{(16 m_c)^2 \sum_{i=1}^9 f^{(i)} F^{(i)}}{(t+Q^2-M_J^2)^2 (u-M_J^2)^2 (s-M_J^2)^2} \end{aligned} \quad (24)$$

In expression (24) we collected all terms containing k_1 and k_2 , the momenta of the decay products of the heavy resonance, in the $F^{(i)}$ factors, all other terms are collected in the $f^{(i)}$ factors. Terms independent of k_1 and k_2 are collected in $f^{(9)}$ with $F^{(9)} = 1$. We have:

$$F^{(1)} = k_1 \cdot g_1 k_2 \cdot g_1 \quad (25a)$$

$$F^{(2)} = k_1 \cdot g_2 k_2 \cdot g_2 \quad (25b)$$

$$F^{(3)} = \frac{1}{2} (k_1 \cdot g_1 k_2 \cdot g_2 + k_1 \cdot g_2 k_2 \cdot g_1) \quad (25c)$$

$$F^{(4)} = L \cdot k_1 L \cdot k_2 \quad (25d)$$

$$F^{(5)} = L \cdot g_1 (L \cdot k_1 g_1 \cdot k_2 + L \cdot k_2 g_1 \cdot k_1) \quad (25e)$$

$$F^{(6)} = L \cdot g_1 (L \cdot k_1 g_2 \cdot k_2 + L \cdot k_2 g_2 \cdot k_1) \quad (25f)$$

$$F^{(7)} = L \cdot g_2 (L \cdot k_1 g_1 \cdot k_2 + L \cdot k_2 g_1 \cdot k_1) \quad (25g)$$

$$F^{(8)} = L \cdot g_2 (L \cdot k_1 g_2 \cdot k_2 + L \cdot k_2 g_2 \cdot k_1) \quad (25h)$$

$$F^{(9)} = 1 \quad (25i)$$

where $L = k_1 + k_2$. The expressions for $f^{(i)}$ can then be written as:

$$\begin{aligned} f^{(1)} = & \frac{1}{2} (L \cdot g_2)^2 (s-Q^2) (s-M_J^2) + \frac{1}{2} L \cdot g_1 L \cdot g_2 (s-M_J^2) (M_J^2-Q^2) \\ & + \frac{1}{4} Q^2 M_J^2 t^2 + \frac{1}{4} (Q^2-u) (s-M_J^2) (M_J^2-Q^2) Q^2 \end{aligned} \quad (26a)$$

$$\begin{aligned} f^{(2)} = & \frac{1}{2} (L \cdot g_1)^2 (u-Q^2) (u-M_J^2) + \frac{1}{2} L \cdot g_1 L \cdot g_2 (u-M_J^2) (M_J^2-Q^2) \\ & + \frac{1}{4} Q^2 M_J^2 t^2 + \frac{1}{4} (Q^2-s) (u-M_J^2) (M_J^2-Q^2) Q^2 \end{aligned} \quad (26b)$$

$$\begin{aligned} f^{(3)} = & -\frac{1}{2} (L \cdot g_1)^2 (Q^2-u) (M_J^2-Q^2) - \frac{1}{2} (L \cdot g_2)^2 (Q^2-s) (M_J^2-Q^2) \\ & + \frac{1}{2} L \cdot g_1 L \cdot g_2 [(M_J^2-Q^2) (M_J-Q^2+t) - 2(s-Q^2) (Q^2-u)] \\ & - \frac{1}{4} Q^2 t (t+M_J^2+Q^2) (M_J^2-Q^2) \end{aligned} \quad (26c)$$

$$f^{(4)} = \frac{1}{8} (s-Q^2) (Q^2-u) [2 Q^2 t + (M_J^2-u) (s-M_J^2)] + \frac{1}{4} Q^4 t^2 \quad (26d)$$

$$f^{(5)} = \frac{1}{8} (Q^2-u) (s-M_J^2) (M_J^2-Q^2) \quad (26e)$$

$$f^{(6)} = -\frac{1}{8} (M_J^2-u) [(Q^2-u) (2 s-Q^2-M_J^2) + 2 Q^2 t] \quad (26f)$$

$$f^{(7)} = -\frac{1}{8} (M_J^2-s) [(Q^2-s) (2 u-Q^2-M_J^2) + 2 Q^2 t] \quad (26g)$$

$$f^{(8)} = \frac{1}{8} (Q^2-s) (u-M_J^2) (M_J^2-Q^2) \quad (26h)$$

$$\begin{aligned} f^{(9)} = & -\frac{1}{16} M_J^2 (L \cdot g_1)^2 [2 Q^2 t^2 + (Q^2-u)^2 (M_J^2-Q^2)] \\ & -\frac{1}{16} M_J^2 (L \cdot g_2)^2 [2 Q^2 t^2 + (Q^2-s)^2 (M_J^2-Q^2)] \\ & + \frac{1}{8} M_J^2 L \cdot g_1 L \cdot g_2 t (M_J^2-M_J^2 Q^2 + Q^2 t) \\ & -\frac{1}{32} M_J^2 Q^2 ((M_J^2 Q^2-su)^2 + (2 t+Q^2-M_J^2) t (M_J^2 Q^2-su) \\ & \quad + t^2 [(M_J^2-Q^2) (M_J^2+t) + (M_J^2-t)^2]) \end{aligned} \quad (26i)$$

Expressions (25) and (26) combined into (24) provide us with the complete modulus squared matrix element for the reaction under consideration.

c) Helicity Amplitudes

In this section we express the inelastic production cross-section in terms of helicity amplitudes (see equation (10)). This does not bring any more information that is not already contained in (21) but provides new insight in the physics of the problem. It is, for example, possible to follow the helicities of the particles involved. We will present explicit expressions in the recoil frame at the constituent level. Rotations to other frames are possible but are more cumbersome than in the covariant approach of the preceding section.

The transition amplitude is written as:

$$M(\gamma^*g_1 \rightarrow Jg_2) = \alpha_S e_q \frac{2\pi}{\sqrt{3M_J}} \psi(0) \delta_{ab} A(\gamma^*g_1 \rightarrow Jg_2) \quad (27)$$

where δ_{ab} indicates that the incoming and the outgoing gluon have to carry the same colour index. The reduced matrix element A is obtained from the six diagrams in figure 2 where the leptonic legs should be removed now. The explicit representation of A is obtained using equation (18):

$$A(\gamma^*g_1 \rightarrow Jg_2) = \frac{64 M_J}{(s-M_J^2)(u-M_J^2)(t-M_J^2+Q^2)} \cdot \\ \cdot \{ \epsilon_1 \cdot \epsilon_1 [0.92 \epsilon_2^* \cdot g_1 \epsilon_J^* \cdot Q - 0.92 g_1 \cdot g_2 \epsilon_2^* \cdot \epsilon_J^* + g_1 \cdot g_2 \epsilon_2^* \cdot Q \epsilon_J^* \cdot g_1] \\ + \epsilon_2^* \cdot \epsilon_J^* [0.92 \epsilon_1 \cdot g_1 \epsilon_1 \cdot g_2 - 0.91 \epsilon_1 \cdot g_2 \epsilon_1 \cdot g_2 + g_1 \cdot g_2 \epsilon_1 \cdot Q \epsilon_1 \cdot g_2] \\ + (Q \leftrightarrow 2) + (1 \leftrightarrow 2) \} \quad (28)$$

where, in an obvious notation, ϵ denotes the polarization vector of the virtual photon, ϵ_J the polarization vector of the heavy resonance and ϵ_1 (ϵ_2) stands for the polarization vector of the incoming (outgoing) gluon. The helicity amplitudes can then be calculated in the usual way. A closed form of the expression is given by*:

*) We use the Jacob-Wick convention.

$$A(\gamma^*g_1 \rightarrow Jg_2) = H_{J\lambda_2; \lambda\lambda_1} = \frac{2 J \ell M_J}{(s+t-Q^2)(-Q^2+M_J^2-t)} \{ (s-Q^2)(\ell-\lambda_1)(J-\lambda_2)(1+\lambda_1\lambda_2 \cos\theta_J) \\ - 2t(1+\cos\theta_J) [J\lambda_1 + \frac{\lambda_1\lambda_2(-Q^2-M_J^2) + \lambda_2\ell(s-Q^2)}{s-M_J^2}] \\ + \frac{(\ell+\lambda_1)(J+\lambda_2)}{s-M_J^2} [(1+\lambda_1\lambda_2)\{(s-M_J^2)(s-Q^2+t) + t(Q^2+t)\}] \\ + (1-\lambda_1\lambda_2)t(s-M_J^2-Q^2+t)] \\ - \frac{2\sqrt{2} \sin\theta_J \ell(1-Q^2)(s-Q^2)}{\sqrt{s}(-Q^2+M_J^2-t)(Q^2+s+t)} \{ (1-\lambda\lambda_1) M_J^2 (1+\lambda_1\lambda_2 \cos\theta_J) \\ + (1+\lambda_1) Q^2 [1+\lambda_1\lambda_2+\lambda_1\lambda_2 \frac{2t M_J^2}{(s-Q^2)(s-M_J^2)}] \} \\ - \frac{\sqrt{-2Q^2}}{s} \frac{2 M_J \sin\theta_J J(1-\ell^2)(s-Q^2)}{(-Q^2+M_J^2-t)(s-Q^2+t)} \{ (1-\lambda_2 J)(1+\lambda_1\lambda_2 \cos\theta_J) \\ + (1+\lambda_2 J) [1+\lambda_1\lambda_2+\lambda_1\lambda_2 \frac{2t M_J^2}{(s-Q^2)(s-M_J^2)}] \} \\ - \frac{4\sqrt{-Q^2}(1-Q^2)(1-\ell^2)}{(-Q^2+M_J^2-t)(-Q^2+s+t)(s-M_J^2)} \{ (1+\lambda_1\lambda_2) [(s-Q^2)(s-M_J^2)(1+\cos\theta_J) + 2 M_J^2 t] \\ + 4 t M_J^2 \cos\theta_J \lambda_1\lambda_2 \} \quad (29)$$

Where J , ℓ , λ_1 and λ_2 denote respectively the helicities of the heavy resonance, virtual photon, incoming gluon and outgoing gluon. θ_J is the angle of the heavy resonance in the constituent center of mass system $\cos\theta_J = \frac{2s}{s-Q^2}$.

In order to facilitate comparison with previous calculations we list the sum over spins of the square of the amplitude (29) in the photoproduction limit ($Q^2 = 0$):

$$\sum_{\text{spins}} |A|^2 = \sum_{J\lambda_2; \lambda\lambda_1} |H_{J\lambda_2; \lambda\lambda_1}|^2 \\ = 8^3 \frac{s^2(s-M_J^2)^2 + t^2(t-M_J^2)^2 + u^2(u-M_J^2)^2}{(s-M_J^2)^2(t-M_J^2)^2(u-M_J^2)^2} M_J^2 ; Q^2 = 0 \quad (30)$$

This reproduces the photoproduction cross-section of Berger and Jones³. Returning to the leptoproduction case, in the limit* $s \rightarrow \infty$ with Q^2, t fixed and $|t| \ll M_J^2$, Q^2 we find a particularly *) In this limit we may have large QCD corrections from higher order terms¹³ of the form $\alpha_S \log(s/|Q^2|)$ or $\alpha_S \log(Q^2/t)$. Nevertheless the qualitative result of helicity conservation and vector meson dominance may be correct.

simple expression for the amplitude (29):

$$\lim_{\substack{s \rightarrow \infty \\ t, Q^2 \text{ fixed} \\ |t| < M_J^2, Q^2}} A(\gamma^* g_1 \rightarrow J g_2) = \frac{4 J \lambda_1 M_J}{M_J^2 - Q^2} (1 + \lambda_1 \lambda_2) (1 + \lambda_2 J) \\ - \frac{8 \sqrt{-Q^2} (1 - J^2) (1 - \lambda_2^2) (1 + \lambda_1 \lambda_2)}{M_J^2 - Q^2} \quad (31)$$

The first term on the right-hand side of (31) is nonvanishing only for

$$\lambda_1 = \lambda_2 = \pm 1$$

$$\lambda = J = \pm 1$$

the second term is nonvanishing only for

$$\lambda_1 = \lambda_2 = \pm 1$$

$$\lambda = J = 0$$

Therefore, in this limit, the amplitude conserves helicity at the subprocess level[†]. The leading s channel helicity amplitudes are

$$H_{++; ++} \sim 16 M_J$$

$$H_{+-; +-} \sim 16 M_J$$

$$H_{+0; +0} \sim -16 \sqrt{-Q^2}$$

Thus the subprocess is s channel helicity conserving and has natural parity exchange⁹. The amplitude (31) also has a vector meson dominance¹⁴ structure due to the factor $(M_J^2 - Q^2)^{-1}$, this factor determines the Q^2 dependence, up to a factor Q in the numerator of the second term on the r.h.s. due to the longitudinal character of the photon in this term.

From the s channel helicity amplitude of the constituent scattering given in equation (29) one can obtain the helicity amplitudes in the hadronic center of mass frame, $H_{\lambda_2 J, \lambda_1 \ell}^{\text{hadron}}$, by boosting along the z axis. The hadronic helicity tensor appearing in equation (16) are then obtained from $H_{\lambda_2 J, \lambda_1 \ell}^{\text{hadron}}$ as

$$H_{JJ'}^{\lambda \lambda'} \sim \sum_{\lambda_1, \lambda_2} H_{\lambda_2 J, \lambda_1 \ell}^{\text{hadron}} H_{\lambda_2 J', \lambda_1 \ell'}^{\text{hadron}}$$

Finally, we would like to make some remarks on the frame dependence of the above expressions. Angular distributions in different frames can be obtained through a rotation, i.e.

[†]To leading order in s this then also holds true at the hadron level.

$$H_{JJ'}^{\lambda \lambda'} = R_{Jjm}^+ (\alpha, \beta, \gamma) H_{mm'}^{\lambda \lambda'} R_{m'j} (\alpha, \beta, \gamma) \quad (32)$$

Such a rotation will only reshuffle terms within the curly brackets of (16). The different frames discussed previously and in the next section can be reached from the above by a rotation around the y axis ($\alpha = \gamma = 0$). Although the rotation matrix has a simple form, the rotation angle itself depends on the kinematic variables of the process in a non-simple manner so that the expressions become quite complicated. It is clear that measurements of the density matrix elements in different frames are only complementary if these measurements are complete since the density matrix elements in different frames are linearly related to each other. In practice these measurements will of course not be complete and a judicious choice of frames is important as discussed previously. Thus, different angular distributions will in general test different aspects of the underlying dynamics.

d) Differential Cross-Section

We now proceed with the study of the differential cross-section. At the level of the subprocess we have:

$$d\sigma = \frac{1}{2S} \frac{d^3 k_2}{(2\pi)^2 2E_2} \frac{d^3 q_2}{(2\pi)^2 2q_{20}} \frac{d^3 k_1}{(2\pi)^3 2k_{10}} \frac{d^3 k_2}{(2\pi)^3 2k_{20}} \\ (2\pi)^4 \delta^4(\ell_1 + g_1 - \ell_2 - g_2 - k_2 - k_1) |M(\ell_1 + g_1 \rightarrow \ell_2 + g_2 + k_1 + k_2)|^2 \quad (33)$$

As four particles appear in the final state we have a twelve-fold differential to start with. Energy-momentum conservation reduces this to 8, one of the azimuthal angles can be integrated over and the two muons have to originate from the heavy resonance, thus fixing their invariant mass. In the end we are thus left with 6 independent variables to describe the process. These are chosen in the following way: three of them are associated in the standard way with the scattered lepton, namely, Q^2 the invariant mass of the virtual photon, $\hat{\phi}$ the energy loss (in the lab. frame) of the lepton and ϕ its azimuthal angle; two other variables specify the angular distribution of the produced muon-pair in the rest frame of the heavy resonance; as a last variable we take t the invariant momentum transfer of the scattered gluon: $t = (g_1 - g_2)^2 = (p_j - Q)^2$. In these variables the cross-section becomes:

$$\frac{d\sigma}{dQ^2 d\hat{\Omega} d\Omega dt} = \frac{\pi}{128 (2\pi)^8 \hat{\Omega}^2 \hat{\nu}} \frac{dp_J^2}{\hat{\nu}} |M(\ell_1+g_1 \rightarrow \ell_2+g_2+k_1+k_2)|^2 \quad (34)$$

where

$$\hat{\Omega} \equiv g \cdot Q \quad (35)$$

$$\hat{\nu} \equiv (\ell_1 + g_1)^2 \quad (36)$$

while Ω refers to the polar and azimuthal angles of the μ^- in the rest frame of the heavy resonance and p_J^2 is the invariant mass of the produced muon pair.

To make contact with hadronic variables we multiply expression (34) with the distribution function for gluons inside the target particle: $G(\xi)$, where ξ is the usual fraction of momentum carried by the gluon in the infinite momentum frame of the target particle:

$$\frac{d\sigma(\ell_1+N \rightarrow N'+\ell_2+k_1+k_2+\dots)}{dQ^2 d\nu d\phi dt d\Omega} = \int_0^1 d\xi G(\xi) \int d\hat{\Omega} \delta(\nu-\hat{\nu}/\xi) \frac{d\sigma(\ell_1+g_1 \rightarrow \ell_2+g_2+k_1+k_2)}{d\hat{\Omega} dQ^2 d\phi dt d\Omega} \quad (37)$$

where $\nu \equiv \hat{\nu}/\xi = p \cdot Q$ is, in the lab frame, the energy loss of the incident lepton times the target mass. Instead of ξ we introduce at this point a more useful variable, z , which in the laboratory frame is the energy of the produced heavy resonance divided by the energy of the exchanged virtual photon:

$$z \equiv \frac{p_{J \cdot p}}{Q^2 \cdot p} = \frac{E_J}{E_{Y^*}} \quad (\text{Lab. frame}) \quad (38)$$

and p is the four-momentum of the target particle (proton or nucleus). The relation between z and ξ is given by

$$z = 1 + \frac{t}{2\nu\xi} \quad (39)$$

In this way we obtain, from (34) and (35), the following expression:

$$\frac{d\sigma(\ell_1+N \rightarrow \ell_2+N' + J + \dots, J \rightarrow k_1+k_2)}{dz d\nu dt dQ^2 d\Omega d\phi} = \frac{\pi g(\xi)}{64 (2\pi)^8 s_1^2} \frac{t}{2(1-z)\hat{\nu}} \frac{dp_J^2}{t} \frac{1}{32} \sum_{\text{spins}} \sum_{\text{colour}} |(\ell_1+g_1 \rightarrow \ell_2+g_2+J, J \rightarrow k_1+k_2)|^2 \quad (40)$$

where

$$\frac{1}{32} \sum_{\text{spins}} \sum_{\text{colour}} |M(\ell_1+g_1 \rightarrow \ell_2+g_2+J; J \rightarrow k_1+k_2)|^2 = \frac{\alpha_S^2 (4\pi)^5}{Q^4 M_J} \frac{\Gamma^2(\frac{J-\mu}{2}) \Gamma(\frac{J+\mu}{2})}{\Gamma(\frac{J+a}{2})} \delta(p_J^2 - M_J^2) \frac{(16\pi\alpha_S)^2}{(t+Q^2-M_J^2)^2 (u-M_J^2)^2 (s-M_J^2)^2} \sum_{i=1}^g f^{(i)} F^{(i)} \quad (41)$$

Use has been made of equations (21), (24) and of the relation

$$\Gamma(J \rightarrow \mu^+ \mu^-) = \frac{16\pi\alpha^2 e^2}{M_J^2} g |\psi(0)|^2 \quad (42)$$

to eliminate $|\psi(0)|^2$. Since u and s are no longer treated as independent variables, they should be replaced in (41) by:

$$s = Q^2 - \frac{t}{1-z} \quad (43)$$

and

$$u = M_J^2 + \frac{zt}{1-z} \quad (44)$$

e) Kinematics

From expressions (40) and (41) we want to calculate the angular distribution of the muonpair in the rest frame of the heavy resonance with reference to the general choice of z axis. All momenta appearing in (25) and (26) therefore have to be expressed in this frame. We start by considering the constituent process in its center-of-mass frame:

$$\begin{aligned}
 Q &= \left(\frac{s-Q^2}{2\sqrt{s}}, \frac{s-Q^2}{2\sqrt{s}}, 0, 0 \right), \\
 g_1 &= \left(\frac{s-Q^2}{2\sqrt{s}}, -\frac{s-Q^2}{2\sqrt{s}}, 0, 0 \right), \\
 p_J &= \left(\frac{s-M_J^2}{2\sqrt{s}}, \frac{s-M_J^2}{2\sqrt{s}} \cos\theta_J, 0, \frac{s-M_J^2}{2\sqrt{s}} \sin\theta_J \right), \\
 k_{1\perp} &= (k_{10}, k_{11}, k_{1\perp} \sin\phi, k_{1\perp} \cos\phi)
 \end{aligned} \tag{45}$$

where ϕ is, as before, the angle between the hadronic plane formed by \vec{Q} and \vec{p}_J and the leptonic plane formed by \vec{k}_1 and \vec{k}_2 (see figure 3). The angle θ_J can be calculated with the help of the variable z :

$$z = \frac{g_1 \cdot p_J}{g_1 \cdot Q} \tag{46}$$

and is given by

$$\cos\theta_J = \frac{s(2z-1) - M_J^2}{s - M_J^2} \tag{47a}$$

$$\sin\theta_J = \frac{2\sqrt{s(1-z)}(sz - M_J^2)}{s - M_J^2} \tag{47b}$$

We next perform a rotation around the x axis to bring \vec{p}_J along the z axis. After this is done we boost the heavy resonance to rest. In this frame the momenta Q , g_1 , g_2 and p_J are given by:

$$Q = \left(\frac{s+M_J^2 - z(s-Q^2)}{2M_J}, \sin\theta_J, 0, -\frac{s-Q^2}{2\sqrt{s}} \sin\theta_J, 0, \frac{s^2+M_J^4 - 2M_J^2 Q^2 - z(s+M_J^2)(s-Q^2)}{2M_J(s - M_J^2)} \right) \tag{48a}$$

$$g_1 = \left(\frac{s-Q^2}{2\sqrt{s}} \left(\frac{z\sqrt{s}}{M_J}, \sin\theta_J, 0, \frac{(M_J^2+s)z - 2M_J^2}{M_J(s - M_J^2)} \sqrt{s} \right) \right) \tag{48b}$$

$$g_2 = \frac{s-M_J^2}{2M_J} (1, 0, 0, 1) \tag{48c}$$

$$p_J = M_J (1, 0, 0, 0) \tag{48d}$$

Since we want to study the angular distribution of the muon pair arising from the decay of the heavy resonance for an arbitrary choice of z axis, we perform one last arbitrary rotation around the y axis. This last rotation will depend on the choice of frame one wants to study. We limit ourselves here to three choices: for the first one we choose the direction

of the virtual photon to fix the z axis, for the second one we choose the opposite of the target direction as z axis and for the third one the hadronic recoil axis, namely $\vec{p}_{\text{Recoil}} = \vec{Q} + \vec{p}$ where \vec{p} is the target momentum. The first choice is the most natural one from the standpoint of the model we are considering. The second one is not completely unambiguous because the constituents can have a certain Fermi motion inside the target and therefore the direction of the target momentum will not always be the same as the direction of the incident constituent. The third frame corresponds to choosing the z axis as the J direction in the hadronic center of mass frame. The recoil momentum, however, does not correspond to the momentum of the recoiling gluon since

$$\vec{p}_{\text{Recoil}} = \vec{Q} + \vec{p} \tag{49}$$

while the momentum of the recoiling gluon g_2 is given by:

$$\vec{g}_2 = \vec{Q} + \epsilon \vec{p}. \tag{50}$$

To reduce the form of the angular distribution in (16) we averaged all quantities over ϕ (see figure 3)*. The expression so obtained has the following general form:

$$\begin{aligned}
 \frac{dN}{d\Omega} &= \frac{3N}{16\pi} \left[1 + \cos^2\theta + A_0 \left(\frac{1}{2} - \frac{3}{2} \cos^2\theta \right) \right. \\
 &\quad \left. + A_1 \sin 2\theta \cos\phi \right. \\
 &\quad \left. + A_2 \frac{1}{2} \sin^2\theta \cos 2\phi \right]
 \end{aligned} \tag{51}$$

where θ and ϕ are the polar and azimuthal angles of one of the decay muons (see also equation (16)). The analytic expressions for N , A_0 , A_1 and A_2 are presented in appendix 1.

*) The angular distribution considered in reference 15 corresponds to $\phi = \phi$ in our notation.

IV. Numerical Results

In the rest frame of the heavy resonance we have taken the plane defined by the target momentum and the virtual photon's momentum as the x-z plane (see equation (47)). The axis are chosen such that all momenta lie in the positive x half plane (see figure 3). The frames are then uniquely fixed by specifying the z axis. The following choices were made:

- beam frame: \vec{Q} along z axis ($\theta_q = 0$)
- target frame: $-\vec{Q}_2$ along z axis ($\theta_2 = \pi$)
- recoil frame: $\vec{Q} + \frac{\vec{Q}_1}{E}$ along z axis.

To evaluate the different coefficients A_0, A_1 and A_2 we integrate (40) over ν, t and z . For simple choices of the gluon distribution function $G(E)$, e.g. the standard form:

$$G(E) = 3 \frac{(1-E)^5}{E} \quad (52)$$

it is possible to do the ν integral (E and ν are related to each other through (39)) analytically because ν only appears in the lepton momenta otherwise. The integrations over z and t were done numerically, the integration limits being the following: for the ν integral, from the constraint

$$0 \leq E \leq 1 \quad (53)$$

and upon comparing ν with $s_T, s_T = (l_1 + p)^2$, one deduces:

$$-\frac{t}{2(1-z)} \leq \nu \leq \frac{s_T}{2} \quad (54)$$

This region becomes narrower if an experimental cut is imposed on the hadronic mass accompanying the heavy resonance:

$$W^2 = (Q + p - p_J)^2 \geq W_0^2 \quad (55)$$

with W_0^2 being typically 5 GeV². In this case the integration region (54) shrinks to

$$-\frac{t - M^2 + W_0^2}{2(1-z)} < \nu < \frac{s_T}{2} \quad (56)$$

M being the target mass. The lower limit of the t integration region can be

deduced from (56):

$$W_0^2 - M^2 - s_T(1-z) \leq t \quad (57)$$

while the upper limit can be calculated from e.g. the transverse momentum squared of the heavy resonance in the constituent center-of-mass frame:

$$p_{J\perp}^2 = sz(1-z) - M_J^2(1-z) \quad (58)$$

and from (43), leading to

$$t \leq Q^2(1-z) - M_J^2 \frac{1-z}{z} \quad (59)$$

(57) and (59) together fix the t -integration region. The last integration is done over the z variable. Combining (57) and (59) gives us a quadratic condition on z :

$$W_0^2 - M^2 - s_T(1-z) \leq Q^2(1-z) - M_J^2 \frac{1-z}{z} \quad (60)$$

solving this gives us the maximal and minimal values of z :

$$\left. \begin{aligned} z_{MAX} \\ z_{MIN} \end{aligned} \right\} = \frac{s_T + Q^2 + M_J^2 - W_0^2 \pm \sqrt{(s_T + Q^2 + M_J^2 - W_0^2)^2 - 4(s_T + Q^2)M_J^2}}{2(s_T + Q^2)} \quad (61)$$

These values do not necessarily correspond to the boundaries of the integration region because it may be experimentally required that the heavy resonance have an energy above a certain minimum value. In particular, in the experiment of the Berkeley-FNAL-Princeton^{15,16} collaboration two regions in z were distinguished: $0.7 < z < 0.9$ and $0 < z < 0.7$. In the first region the resonance picks up a very large fraction of the available energy which makes the reaction look like exclusive heavy resonance production, in the second region the resonance will be accompanied by lots of secondary particles thus making it inelastic. The process described by figure 2 is a priori better suited for the description of the inelastic production of heavy resonances because the accompanying gluon will automatically provide secondaries. We thus expect to have a better description of the data in the $z < 0.7$ region than for z close to 1.

Having performed the integrations over ν, t and z we can now present a discussion of our results.

In the limit $Q^2 = 0$ one finds $A_0 = A_2$. The same result is known to be valid for the QCD diagrams relevant for the Drell-Yan background, namely $q\bar{q} \rightarrow \mu^+\mu^-q$ and $q\bar{q} \rightarrow g\mu^+\mu^-$. It furthermore holds for the hadronic production of X_0 with subsequent decay to a 3S_1 resonance and a photon: $g\bar{g} \rightarrow X_0\gamma$; $X_0 \rightarrow J/\psi\gamma$; $J/\psi \rightarrow \mu^+\mu^-$. A similar relation was found to hold for $e^+e^- \rightarrow J/\psi \rightarrow g\bar{g}$ and $e^+e^- \rightarrow q\bar{q}$ (see references 17 and 18 and references contained therein). As Q^2 increases, deviations from this equality become stronger. Instead of presenting A_0 we plot the parameter α measuring the deviation from isotropy in the polar angle distribution:

$$1 + \alpha \cos^2\theta \quad (62)$$

In figure 5a we see that α is very close to zero in the recoil frame, both for small z and for large z . For large values of Q^2 it becomes more and more negative. In the beam frame (figure 5b) α is around 1/2 for $z < 0.7$ while for larger values of z it is approximately zero with a tendency to turn to negative values for increasing Q^2 . In the target frame (figure 5c) we observe a behaviour which is qualitatively the same as in the beam frame: α is at first very small and tends to become more negative with increasing Q^2 . The value of α has been calculated before in the recoil frame by Baier and Rückl¹, our results agree with theirs.

In figure 6 we plot the Q^2 -dependence of A_1 , the coefficient of the $\sin 2\theta \cos\phi$ term. The qualitative behaviour of A_1 is the same in all frames and does not depend much on the region of z : it is very small and tends to increase for large values of Q^2 .

In figure 7 we present our results for A_2 , the coefficient of the $\sin^2\theta \cos 2\phi$ term. This time for $0.7 < z < 0.9$ we obtain a value around 0.5 for all three frames with A_2 decreasing for large values of Q^2 . For $z < 0.7$ the smallest values for A_2 are found in the beam frame with A_2 changing sign around $Q^2 = 10 \text{ GeV}^2$.

V. Conclusions

The leptoproduction of heavy resonances is interesting because it tests certain basic aspects of our present understanding of the formation of heavy resonances in hadronic processes. In particular if the basic initiating reaction is a two-body collision the leptoproduction process provides a much cleaner situation than the corresponding hadroproduction process: instead of starting from a gluon-gluon collision one has a virtual photon-gluon collision, thus the uncertain gluon distribution function enters linearly in the leptoproduction case while it enters quadratically in the hadroproduction case; furthermore, the number of possible final states is now more limited, e.g. it is not possible to produce directly a X state. The diagrams of figure 2 lead directly to the correct quantum number description of the heavy resonance, this is to be contrasted with models where the production of a free quark-antiquark pair is considered first and then an average description of the production process is made.

We have presented our results for the angular distributions of the produced muon pair in the rest frame of the heavy resonance. The azimuthal angle ϕ of the scattered lepton λ_2 (see figure 1) was integrated over, the remaining angular distribution then has the general form given in equation (51)*. The behaviour of the coefficients A_0 , A_1 and A_2 is presented in figures 5, 6 and 7 for three different choices of z axis. For large values of Q^2 , A_1 and A_2 become negative while the polar angle distribution is not far from being isotropic in most cases. Measurements of these quantities together with measurements of distributions in other kinematic variables should enhance present understanding of the underlying production mechanism.

Acknowledgements

J.C., G.J.G. and M.K. would like to thank Professor K. Gaemers for useful discussions at the early stage of this work. They also thank Professor R. Baier and Dr. R. Rückl for numerous discussions about their results. J.C. and M.K. thank Professor H. Joos of DESY for hospitality while this work was in progress. J.K. would like to thank Dr. J. Gayler and Professor L. Jones for fruitful discussions.

*) The ϕ distribution will be presented in a future publication.

Appendix 1

In this appendix we present the analytic expressions for the functions A_0, A_1, A_2 and N appearing in (51). To this end we first of all decompose the different factors $F^{(k)}$ with $k = 1$ to 9 appearing in equations (25) as follows:

$$F^{(k)} = N_k \left[c_k (1 + \cos^2 \theta) + c_{0k} \left(\frac{1}{2} - \frac{3}{2} \cos^2 \theta \right) + c_{1k} \sin 2\theta \cos \phi + c_{2k} \frac{1}{2} \sin^2 \theta \cos 2\phi + \text{terms depending on } \phi \right] \quad (A1)$$

The terms depending on ϕ are proportional to $\cos 2\phi, \sin 2\phi, \sin \phi$ and/or $\cos \phi$, they disappear upon integration over ϕ . Since we only consider quantities integrated over ϕ we do not write these extra terms explicitly here. The functions A_i ($i = 0, 1$ and 2) appearing in equation (51) can then be obtained as follows:

$$A_i = \frac{g}{\sum_{k=1}^9 N_k c_{ik}} f^{(k)} \quad i = 0, 1 \text{ and } 2 \quad (A2)$$

where the functions $f^{(k)}$ have been given in the main text (see equations 26). The expressions for N_k, c_k and c_{ik} are given in table 1 where the symbol $\langle \dots \rangle$ means taking an average over ϕ :

$$\langle \dots \rangle = \frac{1}{2\pi} \int_0^{2\pi} d\phi \dots \quad (A3)$$

and the explicit form for the four-vector L_μ , defined after equation (25) in the text, is:

$$L_\mu = (k_1 + k_2)_{L_\mu} = (L_0, L_1 \cos \theta_2 + L_3 \sin \theta_2, L_2, -L_1 \sin \theta_2 + L_3 \cos \theta_2) \quad (A4)$$

The angle θ_2 appears here because of the final rotation around the y axis we performed (see text after equation (47)). The different L_i appearing in A4 are given by:

$$L_\mu = \frac{\sqrt{1+\epsilon}}{\sqrt{1-\epsilon}} \left[\begin{array}{l} \frac{s(1-z) + M_J^2 - zQ^2}{2M_J} \\ - \frac{(s+Q^2) \sqrt{(1-z)(sz-M_J^2)}}{s - M_J^2} \\ 0 \\ \frac{(1-z)s^2 - zs(M_J^2+Q^2) + M_J^2(M_J^2 + (2-z)Q^2)}{2M_J(s-M_J^2)} \end{array} \right] + \frac{\sqrt{\epsilon}}{\sqrt{1-\epsilon}} \left[\begin{array}{l} - \frac{[\sqrt{-2Q^2(1-z)(sz-M_J^2)} / M_J] \cos \phi}{(2z-1)s - M_J^2} \frac{\sqrt{-2Q^2} \cos \phi}{\sqrt{-2Q^2} \sin \phi} \\ - \frac{(s+M_J^2) \sqrt{-2Q^2(1-z)(sz-M_J^2)}}{M_J(s-M_J^2)} \cos \phi \end{array} \right] \quad (A5)$$

ϵ is given by equation (6).

The hat ($\hat{\ }$) over the g_i means: $\hat{g}_i \equiv g_i/g_{i0} = (1, \sin \theta_i, 0, \cos \theta_i)$. The angles θ_1 and θ_2 appearing in table 1 are the angles of g_1 and g_2 with respect to the z axis in the frame where the heavy resonance is at rest (see figure 4). In the beam frame where the z axis is given by the direction of the virtual photon's momentum one has

$$\theta_q^B = 0 ; \theta_2^B = \theta_2 - \theta_q ; \theta_1^B = \theta_1 - \theta_q \quad (A6)$$

In the target frame where the z axis is the beam axis

$$\theta_2^T = \pi ; \theta_1^T = \pi + \theta_1 - \theta_2 ; \theta_q^T = \pi + \theta_q - \theta_2 \quad (A7)$$

In the hadronic recoil frame, where the z axis coincides with the hadronic recoil direction one has:

$$\theta_2^R = \theta_2 - \theta_R ; \theta_1^R = \theta_1 - \theta_R ; \theta_q = \theta_q - \theta_R \quad (A8)$$

θ_2^R is the angle between the hadronic recoil direction and the momentum of the recoiling gluon, i.e. the mismatch between the hadronic recoil frame and the constituent recoil frame. This can be calculated in the following way from (49) and (50) one has

$$\vec{P}_{\text{Recoil}} = \frac{1}{\xi} \vec{g}_2 + (1 - \frac{1}{\xi}) \vec{Q} \quad (A9)$$

since \vec{g}_2 and \vec{Q} are explicitly known in the frame under consideration, one can determine the components of \vec{P}_{Recoil} :

$$(P_{\text{Recoil}})_x = \frac{s-Q^2}{s-M_J^2} \sqrt{(1-z)(sz-M_J^2)} \left(\frac{1}{\xi} - 1 \right) \quad (A10)$$

$$(P_{\text{Recoil}})_z = \frac{s-M_J^2}{4sM_J} \left(\frac{s-Q^2}{\xi} + s + Q^2 \right) + \frac{(s-Q^2)(s+M_J^2)(s(2z-1)-M_J^2)}{(s-M_J^2) 4sM_J^2} \left(\frac{1}{\xi} - 1 \right) \quad (A11)$$

It is then a straightforward matter to perform a rotation in the x-z plane such as to align P_{Recoil} along the z direction.

The relative angles $\theta_1 - \theta_2$, $\theta_1 - \theta_q$ and $\theta_2 - \theta_q$ appearing in (A6) and (A7) can be determined from the constituent scattering process. They are given by

$$\cos(\theta_1 - \theta_2) = 1 + \frac{t}{2\omega_1\omega_2} \quad (A12)$$

$$\cos(\theta_1 - \theta_q) = \frac{Q^0}{|\vec{Q}|} - \frac{s-Q^2}{2|\vec{Q}|\omega_1} \quad (A13)$$

$$\cos(\theta_2 - \theta_q) = \frac{Q^0}{M_J^2 - u} - \frac{Q \cdot u}{2|\vec{Q}|\omega_1} \quad (A14)$$

$$\text{with } \omega_1 = \frac{M_J^2 - u}{2M_J} \quad (A15)$$

$$\omega_2 = \frac{s-M_J^2}{2M_J} \quad (A16)$$

$$\text{and } Q_0 = \frac{s+u}{2M_J^2} \quad (A17)$$

References

- 1) R.Baier and R.Rückl, Phys.Lett. 102B, 365 (1981)
- 2) M.B.Einhorn and S.D.Ellis, Phys.Rev.Lett. 34, 1190 (1975); Phys.Rev. D12, 2007 (1975)
- C.E.Carlson and R.Suaya, Phys.Rev. D14, 3115 (1976)
- 3) E.L.Berger and D.Jones, Phys.Rev. D23, 1521 (1981)
- 4) W.Y.Keung, Talk presented at the Z⁰ Physics Workshop, Cornell University, February 1981
- 5) R.Baier and R.Rückl, University of Bielefeld preprint BI-TP 81/30
- 6) H.Fritzsch, Phys.Lett. 67B, 217 (1977)
- M.Glück and E.Reya, Phys.Lett. 79B, 453 (1978);
ibid. 83B, 98 (1979)
- J.P.Levellie and T.Weiler, Nucl.Phys. 814Z, 147 (1979)
- V.Barger, W.Y.Keung and R.J.N.Phillips, Phys.Rev. D20, 630 (1979);
Phys.Lett. 91B, 253 (1980); ibid. 92B, 179 (1980)
- T.Weiler, Phys.Rev.Lett. 44, 304 (1980)
- 7) J.C.Collins and D.E.Soper, Phys.Rev. D16, 2219 (1977)
- 8) J.D.Bjorken and M.C.Chen, Phys.Rev. 154, 1335 (1967)
- 9) K.Schilling and G.Wolf, Nucl.Phys. 861, 381 (1973)
- 10) D.W.Duke and J.F.Owens, Phys.Rev. D23, 1671 (1981)
- 11) J.P.Levellie and T.Weiler, Phys.Rev. D24, 1789 (1981)
- K. Hagiwara, Nucl.Phys. 8173, 487 (1980)
- 12) M.Jacob and G.C.Wick, Annals of Physics 110, 1 (1978)
- 13) B.Humpert and A.C.D.Wright, Annals of Physics 110, 1 (1978)
- 14) J.J.Sakurai and D.Schildknecht, Phys.Lett. 40B, 121 (1972)
- 15) A.R.Clark et al., Phys.Rev.Lett. 45, 2092 (1980)
- M.Strovink, Proceedings of the 1981 International Symposium on Lepton and Photon Interactions at High Energies, Bonn (1981)
- 16) A.R.Clark et al., Phys.Rev.Lett. 43, 187 (1979); ibid. 46, 299 (1981)
- 17) J.Cfeymans, M.Kuroda and G.J.Gounaris, Phys.Lett. 106B, 143 (1981)
- 18) J.G.Körner and D.H.Schiller, DESY preprint 81-043 (July 1981)

Figure Captions

Figure 1: Inelastic leptonproduction of heavy resonance J ($J = J/\psi, Y, \dots$). The model-independent factors are explicitly indicated (see equation 1).

Figure 2: Diagrams used to describe the inelastic leptonproduction of heavy resonance J ($J = J/\psi, Y, \dots$).

Figure 3: k_1 (incident lepton) and k_2 (scattered lepton) define the lepton plane. Q (virtual photon) and J (heavy resonance $J/\psi, Y, \dots$) define the hadron plane. The angle ϕ is the angle between these two planes. Quantities calculated have been averaged over ϕ .

Figure 4: Momenta in the rest frame of the heavy resonance J ($J = J/\psi, Y, \dots$). The momenta of the gluons define the x-y plane. All momenta lie in the positive x half plane.

Figure 5: Values of the coefficient α of the polar angle distribution, $1 + \alpha \cos^2\theta$, integrated over ϕ and Φ (defined in figure 3).

Figure 6: Values of A_1 , coefficient of the $\sin 2\theta \cos\phi$ term in equation (51).

Figure 7: Values of A_2 , coefficient of the $\frac{1}{2} \sin^2\theta \cos 2\phi$ term in equation (51). For $0.7 < z < 0.9$ the values obtained in the target and recoil frames are so close to each other that they overlap in the figure.

Table 1 Caption

The analytic expressions for N_k, c_k and c_{ik} ($k = 1, \dots, 9; i = 0, \dots, 2$) appearing in equation (A1) and (A2).

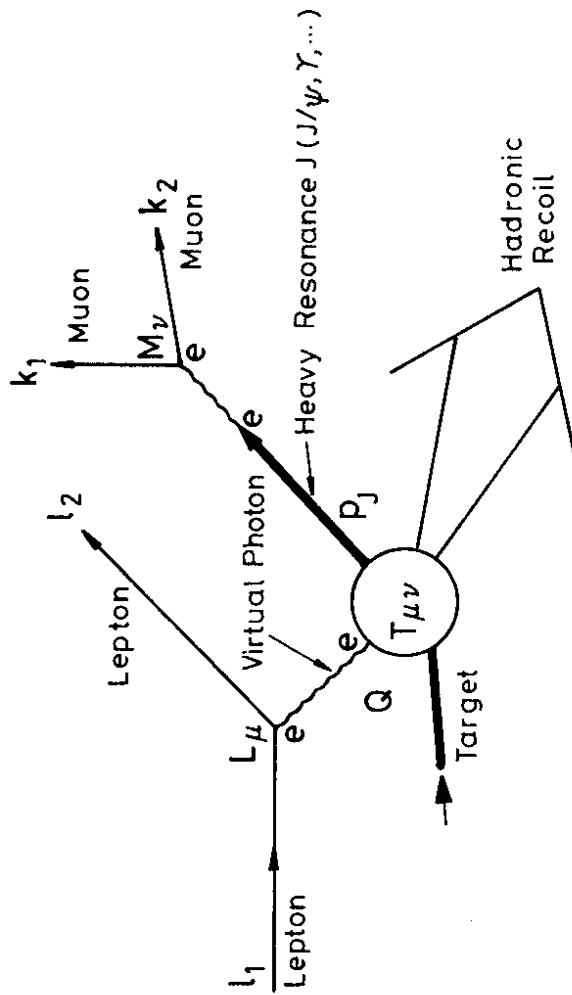
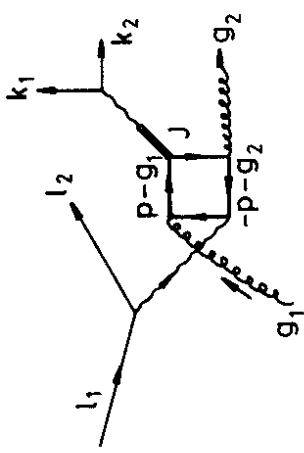


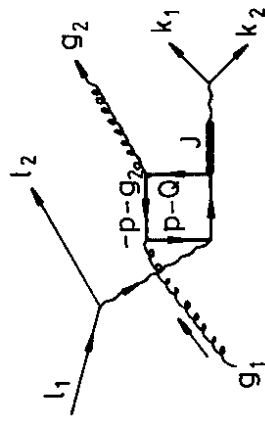
FIGURE 1

k	N_k	C_k	C_{0k}	C_{1k}	C_{2k}
1	$\frac{(M_J^2 - u)^2}{16}$	$\frac{1}{2}$	$\cos^2\theta_1$	$-\sin\theta_1 \cos\theta_1$	$-\sin^2\theta_1$
2	$\frac{(s - M_J^2)^2}{16}$	$\frac{1}{2}$	$\cos^2\theta_2$	$-\sin\theta_2 \cos\theta_2$	$-\sin^2\theta_2$
3	$\frac{(s - M_J^2)(M_J^2 - u)}{16}$	$\frac{1}{4}(3 - \cos(\theta_1 - \theta_2))$	$\frac{1}{2}(1 + \cos(\theta_1 + \theta_2))$	$-\frac{1}{2} \sin(\theta_1 + \theta_2)$	$-\sin\theta_1 \sin\theta_2$
4	$\frac{M_J^2}{4}$	$\frac{\langle L_0^2 \rangle}{2} - \frac{Q^2}{4}$	$\langle L_3^2 \rangle - \frac{Q^2}{2}$	$-\langle L_1 L_3 \rangle$	$\langle L_2^2 - L_1^2 \rangle$
5	$\frac{(M_J^2 - u)^2}{8}$	$\frac{\langle (L\hat{G}_1)L_0 \rangle}{2} + \frac{\langle (L\hat{G}_1)^2 \rangle}{4}$	$\langle (L\hat{G}_1)L_3 \rangle \cos\theta_1 + \frac{1}{2} \langle (L\hat{G}_1)^2 \rangle$	$-\frac{1}{2} \langle (L\hat{G}_1)L_1 \rangle \cos\theta_1 - \frac{1}{2} \langle (L\hat{G}_1)L_3 \rangle \sin\theta_1$	$-\langle (L\hat{G}_1)L_1 \rangle \sin\theta_1$
6	$\frac{(s - M_J^2)(M_J^2 - u)}{8}$	$\frac{\langle (L\hat{G}_1)L_0 \rangle}{2} + \frac{\langle (L\hat{G}_1)(L\hat{G}_2) \rangle}{4}$	$\langle (L\hat{G}_1)L_3 \rangle \cos\theta_2 + \frac{1}{2} \langle (L\hat{G}_1)(L\hat{G}_2) \rangle$	$-\frac{1}{2} \langle (L\hat{G}_1)L_1 \rangle \cos\theta_2 - \frac{1}{2} \langle (L\hat{G}_1)L_3 \rangle \sin\theta_2$	$-\langle (L\hat{G}_1)L_1 \rangle \sin\theta_2$
7	$\frac{(s - M_J^2)(M_J^2 - u)}{8}$	$\frac{\langle (L\hat{G}_2)L_0 \rangle}{2} + \frac{\langle (L\hat{G}_1)(L\hat{G}_2) \rangle}{4}$	$\langle (L\hat{G}_2)L_3 \rangle \cos\theta_1 + \frac{1}{2} \langle (L\hat{G}_1)(L\hat{G}_2) \rangle$	$-\frac{1}{2} \langle (L\hat{G}_2)L_1 \rangle \cos\theta_1 - \frac{1}{2} \langle (L\hat{G}_2)L_3 \rangle \sin\theta_1$	$-\langle (L\hat{G}_2)L_1 \rangle \sin\theta_1$
8	$\frac{(s - M_J^2)^2}{8}$	$\frac{\langle (L\hat{G}_2)L_0 \rangle}{2} + \frac{\langle (L\hat{G}_2)^2 \rangle}{4}$	$\langle (L\hat{G}_2)L_3 \rangle \cos\theta_2 + \frac{1}{2} \langle (L\hat{G}_2)^2 \rangle$	$-\frac{1}{2} \langle (L\hat{G}_2)L_1 \rangle \cos\theta_2 - \frac{1}{2} \langle (L\hat{G}_2)L_3 \rangle \sin\theta_2$	$-\langle (L\hat{G}_2)L_1 \rangle \sin\theta_2$
9	1	$\frac{3}{4}$	$\frac{1}{2}$	0	0

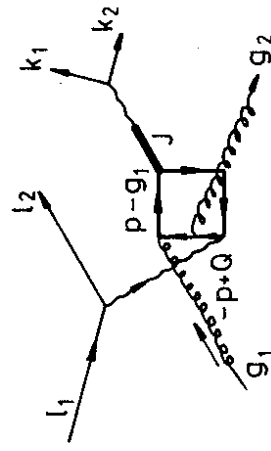
Table 1



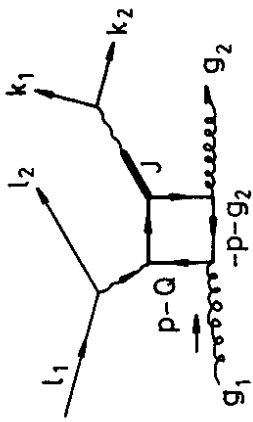
(2d)



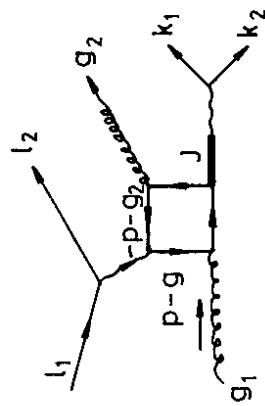
(2e)



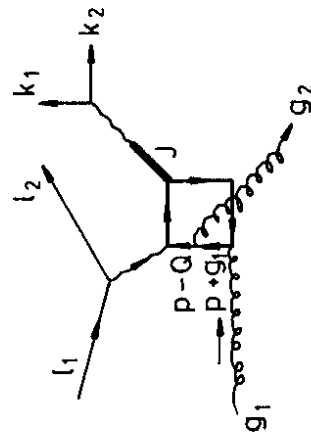
(2f)



(2a)



(2b)



(2c)

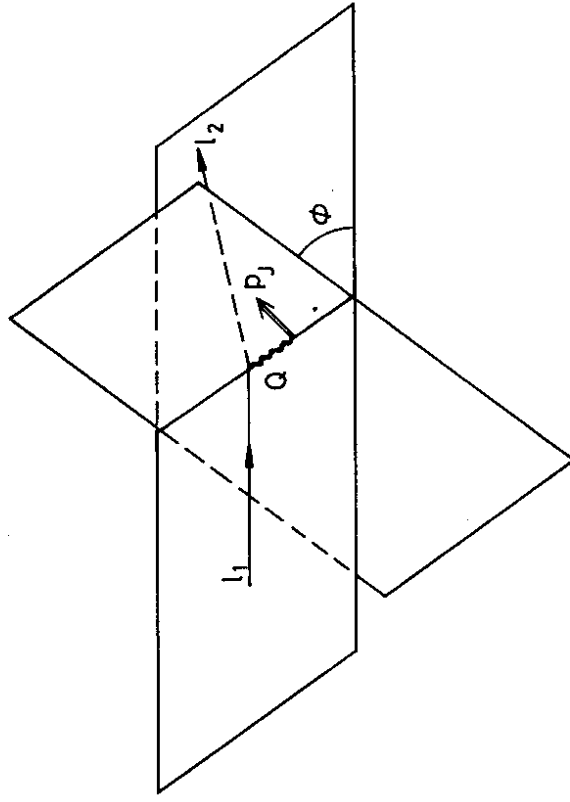


FIGURE 3

FIGURE 2

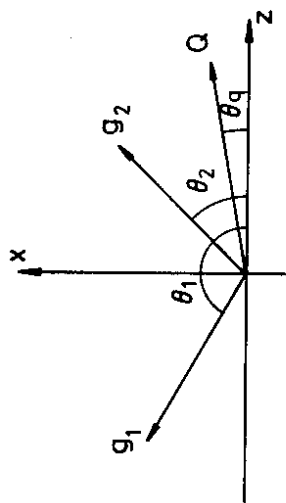


FIGURE 4

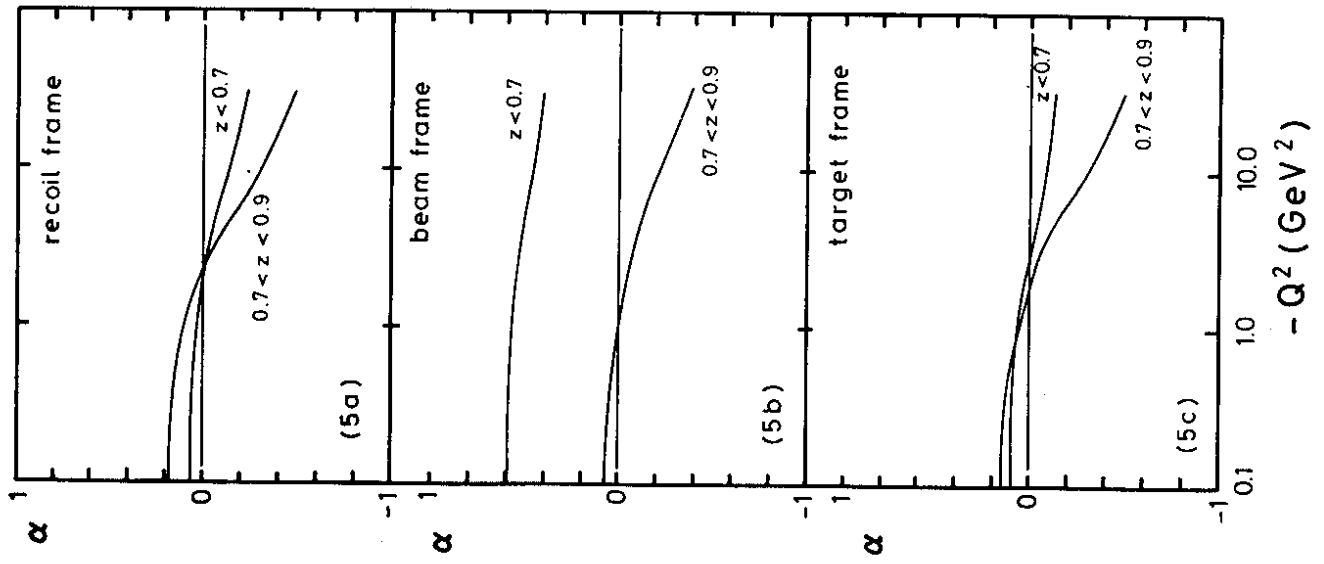


FIGURE 5

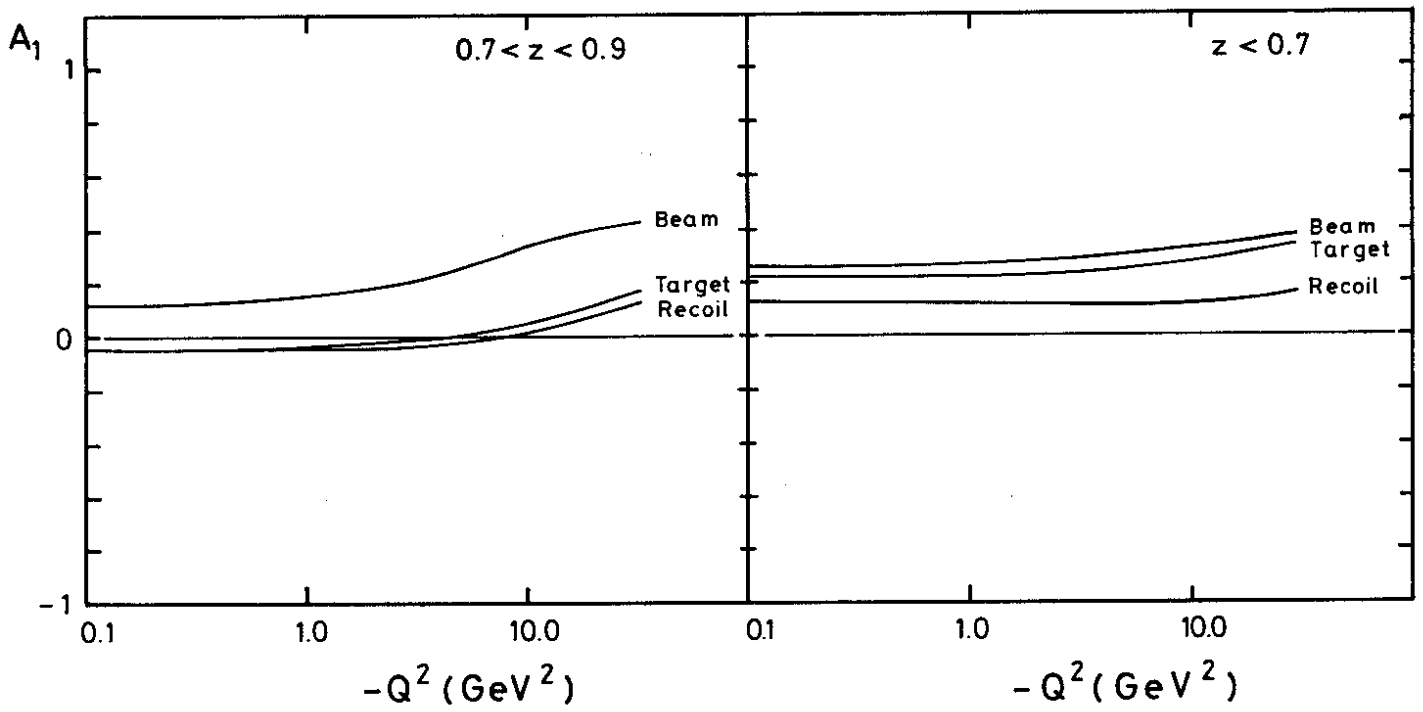


FIGURE 6

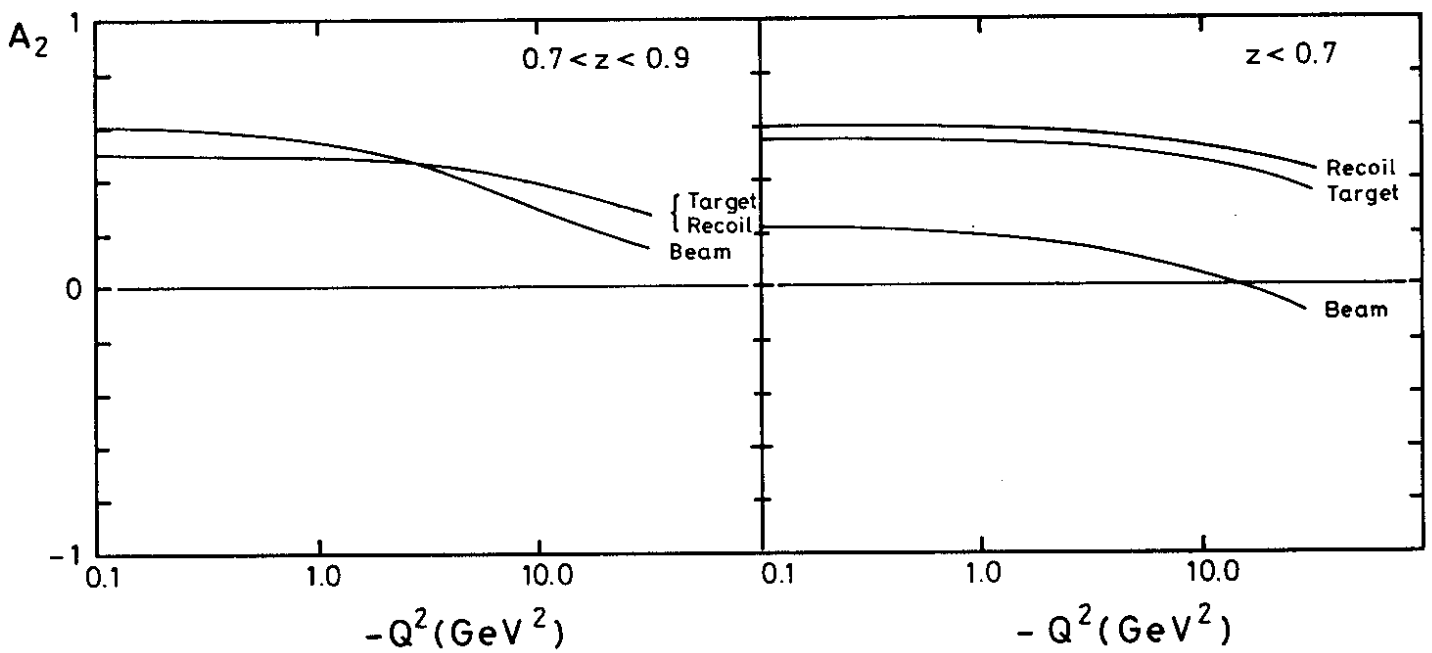


FIGURE 7

